2019-02

Hemizygous UBA5 missense mutation unmasks recessive disorder in a patient with infantile-onset encephalopathy, acquired microcephaly, small cerebellum, movement disorder and severe neurodevelopmental delay

Low, KJ

10.1016/j.ejmg.2018.06.009
European Journal of Medical Genetics
Elsevier BV

European Journal of Medical Genetics 62 (2019) 97–102

Contents lists available at ScienceDirect

European Journal of Medical Genetics

journal homepage: www.elsevier.com/locate/ejmg

Hemizygous *UBA5* missense mutation unmasks recessive disorder in a patient with infantile-onset encephalopathy, acquired microcephaly, small cerebellum, movement disorder and severe neurodevelopmental delay

Karen J. Low[a,*], J. Baptista[b,c], M. Babiker[d], R. Caswell[c], C. King[a], S. Ellard[b,c], I. Scurr[a]

[a] Department of Clinical Genetics, St Michael's Hospital, Bristol, UK
[b] Department of Molecular Genetics, Royal Devon & Exeter NHS Foundation Trust, Exeter, UK
[c] Institute for Biomedical and Clinical Science, University of Exeter Medical School, Exeter, UK
[d] Department of Paediatric Neurology, Bristol Royal Hospital for Children, UK

ARTICLE INFO

Keywords:
UBA5
Ataxia
Infantile-onset encephalopathy
Whole gene deletion

1. Introduction

Ubiquitin-fold modifier 1 (UFM1) is involved in the post-translational modification of proteins and has been implicated in various human diseases (Padala et al., 2017). UFM1 is ubiquitously expressed and has been demonstrated to play a crucial role in cellular stress response and has also been implicated in cancer pathways (Daniel and Liebau, 2014). However the role of the UFM1 cascade in the nervous system is not well understood. In order for proteins to be modified by ufmylation, UFM1 must first be activated by UBA5, a non-canonical E1 activating enzyme, then transferred to an E2 enzyme (UFC1 in the case of UFM1) before final transfer to the protein substrate. Recent studies have shown that UBA5 functions as a dimer and activates UFM1 in a unique *trans*-binding mechanism, whereby one monomer of UBA5 binds both UFM1 and UFC1 via C-terminal regions while the other UBA5 monomer activates the bound UFM1 by adenylation [Oweis et al., 2016].

Duan et al. performed whole exome sequencing (WES) for two Chinese siblings with progressive cerebellar ataxia with non-consanguineous parents and identified compound heterozygote variants in *UBA5* (Duan et al., 2016). The authors elegantly demonstrated that Drosophila knockdown induced motor defects and a shortened lifespan alongside abnormal neuromuscular junctions. Wild type UBA5 restored the neural lesions. Again through WES, Colin et al. (2016) then identified biallelic variants in five children with a pattern of severe intellectual disability, microcephaly, movement disorders, and/or early-onset intractable epilepsy. Studies of fibroblasts from the affected children showed impaired ufmylation with a resulting abnormal endoplasmic reticulum structure. It was also demonstrated that knockdown in zebrafish reduced motility and induced seizure like movements. Muona et al. (2016) reported 9 further individuals with biallelic variants in *UBA5* and a phenotype of severe infantile-onset encephalopathy, dystonia, stagnated development, postnatal microcephaly and spasticity. In this study, CNS-specific knockout of *Ufm1* in mice caused neonatal death accompanied by microcephaly and apoptosis in specific neurons. Most recently Arnadottir et al. (2017) described two sisters with compound heterozygous variants causing early-onset epileptic encephalopathy. Altogether there is now convincing data that the UFM1 cascade is essential for neurodevelopment and that biallelic variants in *UBA5* cause a rare severe phenotypic spectrum which includes infantile onset encephalopathy and movement disorder.

To date all 18 reported cases from 11 families have had biallelic variants in *UBA5*. We report the first case of a UBA5-related neurodevelopmental syndrome in a patient with a whole gene deletion (initially detected on array-CGH) and a missense variant identified by trio exome analysis.

2. Clinical report

This female patient was the first child of a non-consanguineous couple, although there was an older normal male half sibling from a previous relationship. The antenatal and birth history was

* Corresponding author. Department of Clinical Genetics, UHBristol NHS Trust, St Michael's Hospital, Southwell Street, Bristol, BS2 8EG, UK.
E-mail address: Karen.low1@nhs.net (K.J. Low).

https://doi.org/10.1016/j.ejmg.2018.06.009
Received 2 March 2018; Received in revised form 28 May 2018; Accepted 10 June 2018
Available online 12 June 2018

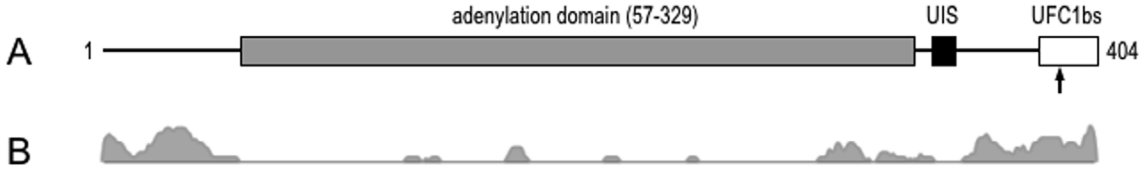

Fig. 1. Functional regions of UBA5. A) Schematic representation of UBA5; annotated according to Oweis et al. (2016); UIS: UFM1-interacting sequence (338–346); UFC1bs: UFC1 binding site (381–404). The arrow indicates the position of aspartate 389. B) Probability of intrinsic disorder (MobiDB-lite data for MobiDB entry Q9GZZ9), plotted on the same horizontal scale as A.

unremarkable. Her growth parameters were all normal at birth including her head size [birthweight was 3.71 kg (0.74SD), length was 53 cm (1.5SD) and head circumference 35 cm (0.9 SD) at term]. However there was parental concern from very early on regarding developmental progress. The child has not yet achieved head control aged 3.5 years. At the age of four months she started to have infantile spasms and her EEG showed hypsarrhythmia. She was treated with high dose steroids resulting in some improvement on subsequent EEGs but the background has remained abnormal. Following the steroid therapy she showed some possible developmental improvement although all areas of development remained significantly delayed. However more recently her development appears to have stagnated. Her epilepsy phenotype includes epileptic spasms, tonic seizures and possible myoclonic seizures. The ketogenic diet was trialled without improvement, but introduction of sodium valproate showed some control of seizure activity. She is gastrostomy fed. At her current age of 3 years and 7 months her weight with gastrostomy feeding is 16.5 kg (0.6 SD) and her height is approximately 98 cm (−0.41 SD). She has an acquired microcephaly with a head circumference of 45 cm (−2.84 SD). Her tone was increased which subsequently improved with antispasticity medication. She was diagnosed with a dyskinetic movement disorder. She has no obvious dysmorphic features. Her brain MRI showed non-progressive lack of volume within the cerebellum with delayed myelination pattern. Her CSF folate level was also noted to be low following a full neurometabolic work up.

3. Methods

3.1. Array-CGH

Copy number analysis was undertaken by oligonucleotide microarray applying the OGT 8 × 60K ISCA v2.0 (GRCh37/hg19) platform and the OGT CytoSure Interpretv4.7 software for data analysis.

3.2. Whole exome sequencing

Genomic DNA samples from the patient and her parents were isolated from peripheral blood samples and enriched for coding sequences using the Agilent SureSelect All Exon v6 system (total target size, 60 Mb; > 23,000 genes). Paired-end reads were sequenced on an Illumina NextSeq 500 sequencer and the data was processed using an in-house pipeline following GATK (v3.4) best practice. Testing was performed as a clinical test in a clinical service laboratory. These results have been uploaded to the DECIPHER database.

3.3. Sanger sequencing

Sanger sequencing was performed for validation of the variant identified by exome sequencing using standard methods. Data was analysed using MutationSurveyor software.

4. Results

Array-CGH showed a *de novo* 597 kb deletion on 3q22.1 described as: arr[GRCh37] 3q22.1(131,875,931_132,472,766)×1 dn which includes the whole *UBA5* gene. The deletion in isolation was thought unlikely to explain the whole clinical presentation and trio exome analysis was carried out given the need for an urgent diagnosis as the patient's mother was pregnant. A *UBA5* missense variant, NM_024818.4: c.1166A > G p.(Asp389Gly) was identified in the patient and her mother. This variant was classified as likely pathogenic according to the ACMG-AMP guidelines (Richards et al., 2015), although analysis with a panel of phenotypic prediction tools returned inconsistent results, with some classifying the variant as pathogenic, some as benign and others classifying it as having an unknown or intermediate effect. The c.1166A > G; p.(Asp389Gly) variant has been reported in a single heterozygote in the gnomAD database [http://gnomad.broadinstitute.org/] (allele frequency, 4.11×10^{-6}), while notably Colin et al. (2016) reported a different variant in the same codon, c.1165G > T; p.(Asp389Tyr), in a patient also carrying a c.778G > A; p.(Val260Met) variant in *trans*. Functional analysis showed the latter variant to exhibit a drastic effect on UBA5 activity, whereas the former had the least effect of any of the variants tested (Colin et al., 2016). The c.1165G > T; p.(Asp389Tyr) variant has also been observed as homozygous in one individual in a Finnish cohort, leading to it being regarded as a hypomorphic allele. Nevertheless, in the case reported by Colin et al., the p.(Val260Met) variant was inherited from the proband's phenotypically normal father, from which it follows that the p.(Asp389Tyr) variant contributed to the phenotype in the proband. This raised the possibility that the p.(Asp389Gly) variant observed in our patient might also contribute to pathogenicity when inherited in combination with a loss of function allele.

We performed various *in silico* analyses to gain insight into the potential effects of the p.(Asp389Gly) and p.(Asp389Tyr) variants on UBA5 structure and function. Aspartate 389 lies in the extreme C-terminal of UBA5 which has been shown to be required for UFC1 binding (Oweis et al., 2016) (Fig. 1A), but which is missing from all previously reported crystal structures of UBA5, presumably due to flexibility within protein crystals. Consistent with this, the MobiDB database (Piovesan et al., 2018) reports that both the extreme N- and C-termini of UBA5 have high probability for intrinsic disorder (Fig. 1B). A

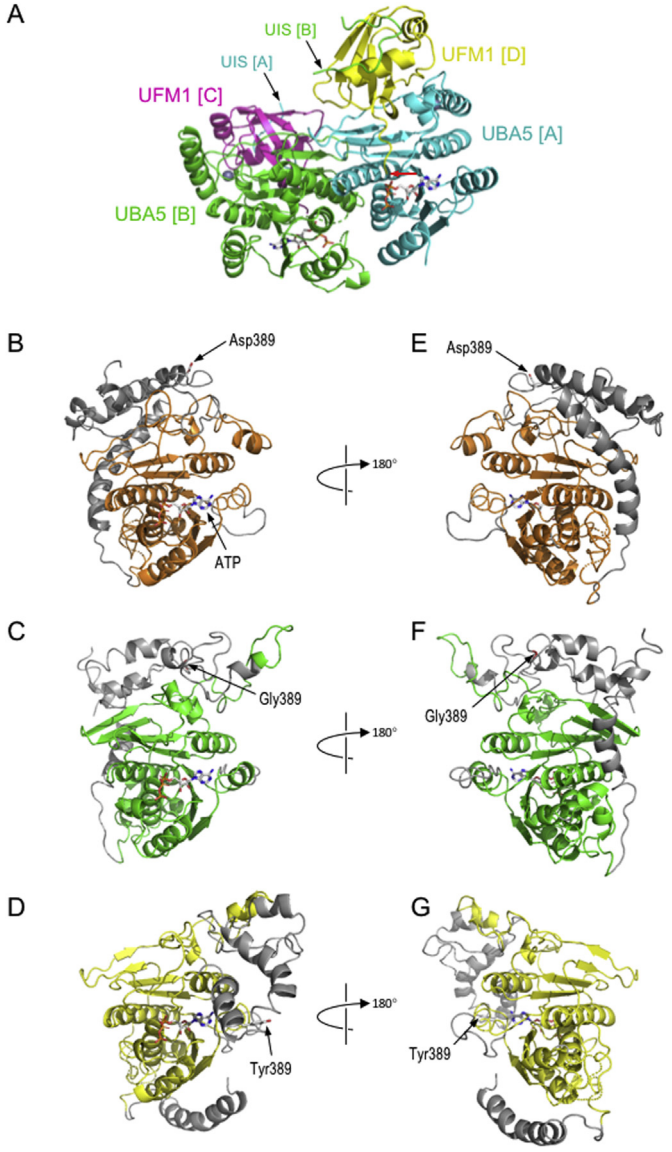

Fig. 2. Actual and predicted structures of UBA5. A) Structure of the UBA5-UFM1 heterotetramer, as determined by Oweis et al. (PDB id 5iaa); for reference, the ATP ligand from crystal structure 3h8v (UBA5 residues 69–318) is superimposed within the ATP binding cleft in both UBA5 monomers. In the *trans*-binding mechanism, UFM1 chain D [yellow] is bound by the UIS of UBA5 chain B [green] A but activated at its C-terminus by adenylation catalysed by UBA5 chain A [turquoise], and *vice versa*; the red arrow indicates the position of the C-terminus of UFM1 chain D proximal to the α-phosphate group of ATP. Note that in this structure the flexible linker between the adenylation domain and UIS of UBA5 (residues 323–332) and residues C-terminal of the UIS were not resolved. B) Phyre2-predicted structure of full-length UBA5 (residues 1–404); regions of high confidence (templated) prediction are coloured orange, while those of low confidence are grey; the position of Asp389 is indicated. C, D) As A, but showing predicted structures of the p.(Asp389Gly) and p.(Asp389Tyr) variants respectively; green or yellow colouring indicates regions of high confidence prediction. E-G) As B-D respectively, but rotated 180° about the vertical axis. (For interpretation of the references to colour in this figure legend, the reader is referred to the Web version of this article.)

search for structural templates for comparative modelling of this region of UBA5 failed to identify any suitable candidates (data not shown). Consequently, further analysis relied on a combination of 3D structural predictions using *ab initio* modelling, and other predictions based on amino acid sequence alone.

For 3D modelling, the full-length sequences of UBA5 and the p.(Asp389Gly) and p.(Asp389Tyr) variants were submitted to the Phyre2 server (Kelley et al., 2015) for modelling in intensive mode, which provides a combination of both multi-templated comparative modelling (where suitable structural templates exist) and *ab initio* modelling based on sequence alone. It should be noted however that the latter remains of low reliability and predictions over such regions should be regarded with caution. Within regions of high confidence prediction, the Phyre2 model for full-length UBA5 showed strong similarity with previously published structures for the adenylation domain (Piovesan et al., 2018) (Fig. 2A and B). Low-confidence modelling of the extreme C-terminal region predicted this to be folded back across one of the surfaces occupied by UFM1 in the UBA5-UFM1 complex, and both the p.(Asp389Gly) and p.(Asp389Tyr) variants resulted in profound changes to the predicted structure of this region (Fig. 2B–D). Further modelling using the I-TASSER server (Yang et al., 2015), which similarly combines multi-templated and *ab initio* modelling, returned models which closely resembled those from Phyre2 over the adenylation domain, but which differed considerably outside this region. However, like Phyre2, I-TASSER predicted substitutions at residue 389 to have a profound effect on structure (Figs. S1A and B). Taken together, these results suggests that while *ab initio* modelling cannot yet provide a reliable model for the structure of the C-terminal region of UBA5, both the p.(Asp389Gly) and p.(Asp389Tyr) variants have a calculable effect on the predicted structure.

The low confidence of modelling of the C-terminal region reflects the predicted disorder of this region (Fig. 1A). Such regions are extremely common in proteins and their inherent flexibility allows them to form weak but dynamic interactions with multiple binding partners (Uversky et al., 2008). However, such regions by definition lack intrinsic secondary structure and thus are recalcitrant to structural analysis both *in vitro* and *in silico*, although a number of algorithms for prediction of regions of intrinsic disorder have been developed. Analysis of reference and variant UBA5 sequences using the MetaDisorder algorithm (Yachdav et al., 2014) showed that both the p.(Asp389Gly) and p.(Asp389Tyr) variants caused a significant decrease in predicted disorder around the position of the substitution (Fig. 3), which might affect flexibility in this region of the protein. Furthermore, since regions of intrinsic disorder are usually exposed to solvent they contain a high proportion of charged and polar amino acids (Uversky et al., 2008), and substitutions which increase the hydrophobicity are likely to adversely affect the properties of such regions. The changes in hydrophobicity index for the p.(Asp389Gly) and p.(Asp389Tyr) variants are +3.1 and + 2.2 respectively (Kyte-Doolittle scale; range = −4.5 [arginine, most polar], to +4.5 [isoleucine, most hydrophobic] (Kyte and Doolittle, 1982)), suggesting that both substitutions will be thermodynamically unfavourable.

5. Discussion

This case provides further evidence that biallelic variants in *UBA5* are associated with epileptic encephalopathy, developmental delay/stagnation, acquired microcephaly, intellectual disability, movement disorder and cerebellar atrophy with ataxia. Our case is the first

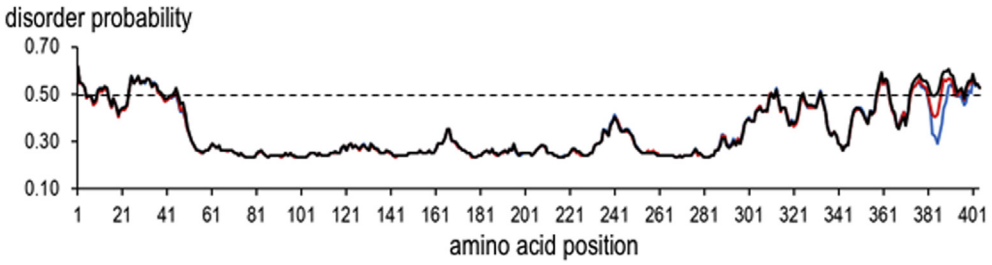

Fig. 3. Effect of Aspartate 389 substitutions of predicted intrinsic disorder. Results are shown for Meta-Disorder prediction of probability for intrinsic disorder in full-length UBA5 (black line) or the p.(Asp389Gly) and p.(Asp389Tyr) variants (red and blue lines respectively); the dashed horizontal line indicates the threshold of 0.5, above which regions are called as disordered. (For interpretation of the references to colour in this figure legend, the reader is referred to the Web version of this article.)

example in which whole gene deletion of UBA5 contributes to the phenotype, and is consistent with previous work which demonstrated that knockdown studies in Drosophila, Zebrafish and Mice lead to severe neurological phenotypes which overlap those seen in humans. The effect of the second variant, a missense p.(Asp389Gly) substitution, is somewhat harder to interpret, and indeed some phenotypic prediction tools classified this variant as benign. Phylogenetic analysis indicates that while aspartate is the most commonly-occurring amino acid at this position, this residue has only low evolutionary conservation with glycine being present at the same position in a small number of aligned sequences. However, all such sequences are derived from invertebrate homologues; moreover, the motif Thr-Val-Glu-Asp-Ser (residues 386–390) which is invariant in mammals differs at every position in these invertebrate sequences, suggesting that compensating variation (and possibly diversification of function) has arisen in *UBA5* during speciation. Furthermore, whereas it would generally be expected that regions of low evolutionary conservation would have a higher density and frequency of missense variants in the gnomAD database, this is not true for the C-terminal of UBA5, for which variation in the human population is no higher than over the entire gene. This indicates that this region is under similar constraint as other coding regions within *UBA5* and that tools which rely heavily on phylogenetic analysis may be unreliable in such cases. In contrast, the rarity of the p.(Asp389Gly) variant in the gnomAD database, and the fact that a different variant at the same position has been shown to contribute to pathogenicity when inherited in combination with the more damaging p.(Val260Met) variant, are supportive of a role for the variant in pathogenicity. *In silico* analyses suggest that both the p.(Asp389Gly) and p.(Asp389Tyr) variants alter the properties of the intrinsically-disordered C-terminal region, suggesting a possible common mechanism whereby these variants affect the interaction with UFC1 for which the C-terminal region of UBA5 is essential. Taken together, the rarity of the p.(Asp389Gly) variant and the fact that a different pathogenic variant has been reported at the same position suggests that the combination of missense variant and loss of function allele are indeed responsible for the phenotype in our patient; however, we cannot formally exclude the possibility that other variants, for example non-coding variants which compromise the expression of the functional allele, might also be responsible.

The phenotype of all 18 reported cases, along with this new case, are summarised in Table 1. With the exception of siblings reported by Duan et al. who are described as having childhood onset with cataract and normal intelligence, the phenotype is highly consistent, with all 17 remaining cases having severe ID and microcephaly. The similarity of the phenotype in our patient further supports our conclusion that the biallelic mutations identified in *UBA5* are causative in this case. Spasticity, movement disorder and epilepsy are described in all but two of the 17 patients. Cerebellar and cortical atrophy or hypoplasia is described in most, with a thin corpus callosum and delayed myelination being a recurrent finding on Brain MRI. 14 of the patients had the c.1111G > A; (p.Ala371Thr) variant which may represent a mutational hotspot.

When the array-CGH abnormality was detected we consulted the DECIPHER database (Firth et al., 2009) to assess whether there were other reported patients with overlapping genotypes/phenotypes. We note that there are multiple patients with deletions overlapping this locus. It is key that patients with such microarray abnormalities are phenotyped carefully and if they fit in to this neurological spectrum then *UBA5* should be sequenced to look for the second hit. This is not only important for accurate diagnosis and management but also for accurate genetic counselling for families who may have a 25% recurrence risk.

Early onset epileptic encephalopathy can be caused by variants in multiple genes (Trump et al., 2016) and is therefore a non-specific phenotype on its own. However the combination of acquired microcephaly, a movement disorder and an abnormal cerebellum are a specific pattern to *UBA5* and should alert clinicians to test for this diagnosis in early onset encephalopathies and cases of severe neurodevelopmental delay.

6. Conclusions

Biallelic variants in *UBA5* cause a specific syndrome of early onset epileptic encephalopathy with developmental delay, acquired microcephaly, abnormal cerebellum and movement disorder. Whole gene deletions of one allele in combination with a pathogenic variant on the other allele can cause the same syndrome and may be picked up initially through microarray CGH. Given the genetic counselling and diagnostic implications, *UBA5* should be tested in patients presenting with this pattern of features.

Conflicts of interest

None of the authors have received any specific funding towards the work in this paper nor have any conflicts of interest.

Table 1
Clinical and genetic features of the reported patient along with all UBA5 patients published to date.

Individual	1	Muona et al., 2016						
		A4	A6	B3	B5	B8	B10	C4
cDNA (NM_003632.2)	c.1166A > G/c.(?_-1041)_(*1581_?)	c.164G > A/c.1111G > A	c.164G > A/c.1111G > A	c.855C > A/c.111G > A	c.855C > A/c.111G > A	c.855C > A/c.111G > A	c.855C > A/c.111G > A	c.562C > T/c.1111G > A
Protein	(p.Asp389Gly)/(p.Met1_Met1211del	(p.Arg55His)/(p.Ala371Thr)	(p.Arg55His)/(p.Ala371Thr)	(p.Tyr285Ter)/(p.Ala371Thr	(p.Tyr285Ter)/(p.Ala371Thr	(p.Tyr285Ter)/(p.Ala371Thr	(p.Tyr285Ter)/(p.Ala371Thr	(p.Arg188Ter)/(p.Ala371Thr)
Lethal		+			+	+	+	
Sex	female	male	female	female	male	male	male	male
Severe Early Irritability	+	+	+	+	+	+	+	+
Movement disorder	+	+	+	+	+	+	+	+
Severe ID	+	+	+	+	+	+	+	+
Postnatal Microcephaly	+	+	+	+	+	+	+	+
Epilepsy in infancy	+	+	+	+	+	+	+	+
Myoclonic jerks	+	+	+	+	+	+	+	
Infantile spasms	+	+	+	+	+	+	+	+
Spasticity	+	+	+	+	+	+	+	+
Hypotonia		+	+	+	+	+	+	+
Gait ataxia								
Dysarthria								
Progressive growth failure				+	+	+	+	
Cerebellar loss of volume	+	performed in 7/9 and abnormalities included cerebellar and cortical atrophy						
Vision								

Individual	Muona et al., 2016		Duan et al., 2016		Colin et al., 2016				
	D3	E3	II:2	II:3	A:II-1	A:II-2	B:II-2	C:II-1	D:II-2
cDNA (NM_003632.2)	c.181C > T/c.1111G > A	c.562C > T/c.1111G > A	c.568C > T/c.760A > G	c.568C > T/c.760A > G	c.1111G > A/c.904C > T	c.1111G > A/c.904C > T	c.1111G > A/c.971_972insC	c.778G > A/c.1165G > T	c.169A > G/c.503G > A
Protein	(p.Arg61Ter)/(p.Ala371Thr)	(p.Arg188Ter)/(p.Ala371Thr)	(p.R246X)/(p.K310E)	(p.R246X)/(p.K310E)	(p.Ala371Thr)/(p.Gln302*)	(p.Ala371Thr)/(p.Gln302*)	(p.Ala371Thr)/(p.Lys324Asnfs*14)	(p.Val260Met)/(p.Asp389Tyr)	(p.Met57Val)/(p.Gly168Glu)
Lethal									
Sex	female	male	female	male	male	male	female	female	female
Severe Early Irritability	+	+							
Movement disorder	+	+			+			+	+
Severe ID	+	+			+	+	+	+	+
Postnatal Microcephaly	+	(-2SD)			+	+	+	+	+
Epilepsy in infancy		+			+	+	+		
Myoclonic jerks									
Infantile spasms									
Spasticity	+	+			+	+			+
Hypotonia	+	+			+	+	+	+	+
Gait ataxia			+	+					
Dysarthria			+	+					
Progressive growth failure		+	in childhood but achieved normal adult size	in childhood but achieved normal adult size	+	+	+	+	+
Cerebellar loss of volume	performed in 7/9 and abnormalities included cerebellar and cortical atrophy		+	+	thin corpus callosum		thin corpus callosum	+	cortical and cerebellar atrophy, thin corpus callosum
Vision			cataract	cataract	vision defect	vision defect	vision defect	vision defect	vision defect

Appendix A. Supplementary data

Supplementary data related to this article can be found at http://dx.doi.org/10.1016/j.ejmg.2018.06.009.

References

Arnadottir, G.A., Jensson, B.O., Marelsson, S.E., et al., 2017. Compound heterozygous mutations in UBA5 causing early-onset epileptic encephalopathy in two sisters. BMC Med. Genet. 18 (1), 103.

Colin, E., Daniel, J., Ziegler, A., et al., 2016. Biallelic Variants in UBA5 reveal that disruption of the UFM1 cascade can result in early-onset encephalopathy. Am. J. Hum. Genet. 99, 695–703.

Daniel, J., Liebau, E., 2014. The ufm1 cascade. Cells 3, 627–638.

Duan, R., Shi, Y., Yu, L., et al., 2016. UBA5 mutations cause a new form of autosomal recessive cerebellar ataxia. PLoS One 11 (2), e0149039.

Firth, H.V., Richards, S.M., Bevan, A.P., et al., 2009. DECIPHER: database of chromosomal imbalance and phenotype in humans using ensembl resources. Am. J. Hum. Genet. 84, 524–533.

Kelley, L., Mezulis, S., Yates, C., et al., 2015. The Phyre2 web portal for protein modeling, prediction and analysis. Nat. Protoc. 10, 845–858.

Kyte, J., Doolittle, R.F., 1982. A simple method for displaying the hydropathic character of a protein. J. Mol. Biol. 157 (1), 105–132.

Muona, M., Ishimura, R., Laari, A., et al., 2016. Biallelic variants in UBA5 link dysfunctional UFM1 Ubiquitin-like modifier pathway to severe infantile-onset encephalopathy. Am. J. Hum. Genet. 99, 683–694.

Oweis, W., Padala, P., Hassouna, F., Cohen-Kfir, E., Gibbs, D.R., Todd, E.A., Berndsen, C.E., Wiener, R., 2016. Trans-binding mechanism of ubiquitin-like protein activation revealed by a UBA5-ufm1 complex. Cell Rep. 20;16 (12), 3113–3120.

Padala, P., Oweis, W., Mashareh, B., et al., 2017. Novel insights into the interaction of UBA5 with UFM1 via a UFM1-interacting sequence. Sci. Rep. 7 (1), 508.

Piovesan, D., Tabaro, F., Paladin, L., Necci, M., Micetic, I., Camilloni, C., Davey, N., Dosztányi, Z., Mészáros, B., Monzon, A.M., Parisi, G., Schad, E., Sormanni, P., Tompa, P., Vendruscolo, M., Vranken, W.F., Tosatto, S.C.E., 2018. MobiDB 3.0: more annotations for intrinsic disorder, conformational diversity and interactions in proteins. Nucleic Acids Res. 4;46 (D1), D471–D476.

Richards, S., Aziz, N., Bale, S., Bick, D., et al., 2015. ACMG laboratory quality assurance committee. Standards and guidelines for the interpretation of sequence variants: a joint consensus recommendation of the american college of medical genetics and genomics and the association for molecular pathology. Genet. Med. 17 (5), 405–424.

Trump, N., McTague, A., Brittain, H., et al., 2016. Improving diagnosis and broadening the phenotypes in early-onset seizure and severe developmental delay disorders through gene panel analysis. J. Med. Genet. 53 (5), 310–317.

Uversky, V.N., Oldfield, C.J., Dunker, A.K., 2008. Intrinsically disordered proteins in human diseases: introducing the D2 concept. Annu. Rev. Biophys. 37, 215–246.

Yachdav, G., Kloppmann, E., Kajan, L., et al., 2014. PredictProtein - an open resource for online prediction of protein structural and functional features. Nucleic Acids Res. 42 (Web server issue) W337–343.

Yang, J., Yan, R., Roy, A., et al., 2015. The I-TASSER Suite: protein structure and function prediction. Nat. Methods 12, 7–8.

Web resources

Phyre2: http://www.sbg.bio.ic.ac.uk/phyre2/html/page.cgi?id=index.

I-TASSER: https://zhanglab.ccmb.med.umich.edu/I-TASSER/.

PredictProtein: https://www.predictprotein.org/.

MobiDB: http://mobidb.bio.unipd.it/.